Spectroscopic study of structural defects caused by oxygen vacancies in solid solutions of stabilized zirconium dioxide

© P.A. Ryabochkina [1], V. Pankratov [2], E.E. Lomonova [3], N.V. Sidorova [1], S.A. Artemov [1], M.V. Gerasimov [1]

[1] National Research Ogarev Mordovia State University, Saransk, Russia
[2] Institute of Solid State Physics, University of Latvia,
LV-1063 Riga, Latvia
[3] Prokhorov Institute of General Physics, Russian Academy of Sciences, Moscow, Russia

e-mail: ryabochkina@freemail.mrsu.ru

Using spectral-luminescent methods upon excitation by synchrotron radiation, structural defects caused by oxygen vacancies were revealed in ZrO_2-Y_2O_3-Ho_2O_3, ZrO_2-Y_2O_3-Er_2O_3, ZrO_2-Y_2O_3 crystals. The positions of the energy levels of oxygen vacancies V^{+1} and V^{+2} located near the conduction band are determined.

Keywords: zirconium dioxide, rare earth ion, oxygen vacancy, luminescence spectra, excitation spectra, synchrotron radiation.

Introduction

Spectroscopic properties of the crystals of stabilized zirconium dioxide that are doped with rare-earth (RE) ions substantially differ from properties of many laser materials with an ordered structure. Due to its disorder crystal structure, the cubic crystals of stabilized zirconium dioxide have several kinds of the optical centers of the RE activator ion, which differ in the nearest crystal environment. Due to superposition of the spectra of the various optical centers of the activator ions, their absorption and luminescence spectra are heterogeneously broadened. It makes it possible to consider these crystals as active laser media which are frequency retunable and designed to generate short pulses [1–8].

The cubic crystals of stabilized zirconium dioxide are solid solutions ZrO_2 with oxides of the II (Ca, Mg) and III (Y, Sc) groups of the periodic table. The kind and concentration of the stabilizing oxide in the solid solution influence the crystal and electron structure of the crystals.

The experiments for obtaining laser generation are most often conducted on the crystals ZrO_2-Y_2O_3 doped with the RE ions. With heterovalent substitution of the ions Zr^{4+} with the ions Y^{3+} (RE^{3+}), oxygen vacancies (defects) are formed in a number required for compliance with a condition of electrical neutrality.

In the papers [7,8], we have reported obtaining two-micron pulse generation at the transition $^5I_7 \rightarrow {}^5I_8$ of the ions Ho^{3+} in the crystals ZrO_2-Y_2O_3-Ho_2O_3 in Q-switched mode when pumping the ions Ho^{3+} by means of the continuous thulium fiber laser [7] and the continuous solid-state laser on the crystals $LiYF_4$:Tm [8] to the level $^5I_7$. In the series of the generation experiments for obtaining pulse generation in Q-switched mode on the crystals ZrO_2- Y_2O_3-Ho_2O_3, it has been established [9] that for the laser generation pulse of the duration of 46 ns and the repetition frequency of 1 kHz, when the peak power density is 196 MW/cm^2, the butt ends of the active elements exhibit „burn ups". Within the framework of a series of the studies aimed at identifying the influence of quality of crystal surface processing, as performed by the authors [8], it has been established that the butt ends were clearly damaged in all the modes used for surface processing of the active elements, including chemical & mechanical polishing.

Fig. 1 shows pictures of the „burn ups", which occurred at the butt ends of the active elements made of the crystals ZrO_2-13.6mol.%Y_2O_3-0.4mol.%Ho_2O_3, during the experiments for obtaining laser generation in Q-switched mode.

As shown in the papers [10–14], the anion vacancies in the zirconium dioxide crystals can by characterized by energy level in the band gap, including near the conduction band's bottom, depending on the number of electrons captured by them. We have assumed that at the high density pumping powers, there was significantly increased probability of upconversion processes between the ions Ho^{3+} which cause population of excited high energy levels of these ions. The presence of defects related to the oxygen vacancies and characterized by the energy levels in the crystals' band gap, and their interaction with the excited ions Ho^{3+} result in electron population of the energy levels of the defects near the conduction band and subsequent thermally induced transition of these electrons into the conduction band. Electrons appearing in the conduction band and interacting with the radiation field of laser generation result in electrical breakdown at the butt ends of the active element made of the crystal ZrO_2-Y_2O_3-Ho_2O_3.
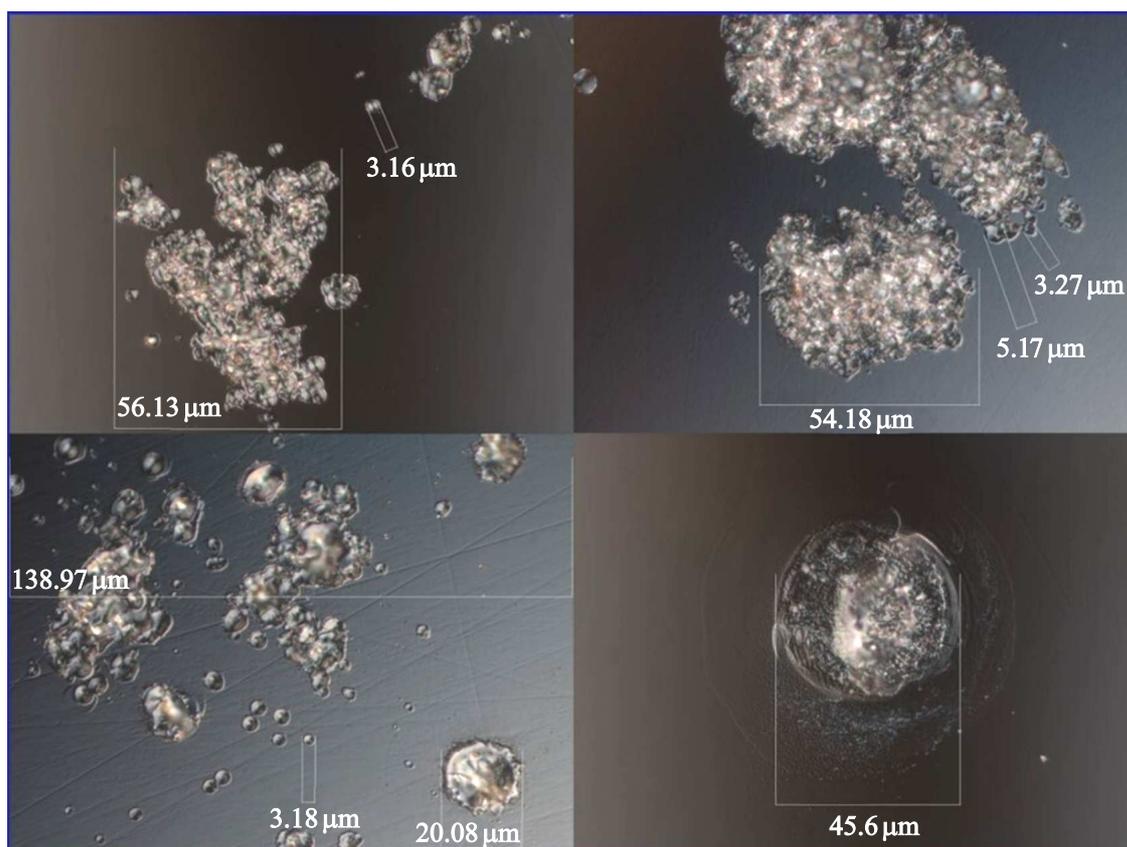
Figure 1. Images of the „burn ups" at the butt ends of the active elements after the generation experiment, as obtained using the optical microscope Carl Zeiss Axio Imager Z2 Vario.

The present study was aimed at experimentally confirming existence of the defects occurring due to the oxygen vacancies and having characteristic energy levels within the crystals' conduction band. ZrO_2-Y_2O_3−Ho_2O_3, ZrO_2-Y_2O_3−$Er2O3$, ZrO_2-Y_2O_3.

Description of research objects and experimental techniques

The crystals of the compositions ZrO_2-15mol.%Y_2O_3, ZrO_2-13.6mol.%Y_2O_3-0.4mol.%Ho_2O_3, ZrO_2-13.4mol.%Y_2O_3-0.6mol.%Er_2O_3 were synthesized by directional crystallization of a melt by direct high-frequency heating in the cold container of the diameter of 130 mm at the growth rate of 10 mm/h using the unit „Kristall-407".

The luminescence spectra and the excitation spectra were recorded by synchrotron radiation using the Finnish-Estonian line FinEstBeAMS of the synchronous center MAX IV (Lund, Sweden) [15]. The line FinEstBeAMS is designed for interdisciplinary studies and contains several terminal stations at two branches. One of them is a compact unit for low-temperature luminescence research FINESTLUMI [16,17]. The unit FINESTLUMI is equipped with two secondary monochromators and is designed to

detect luminescence in the ultraviolet (UV), visible and near infrared (NIR) ranges of the spectrum (200−1500 nm) using the spectrometer Andor Shamrock (SR-303i). The spectrometer has two output ports with a CCD detector and a photomultiplier, respectively. Depending on a spectrum region of the recorded signal, it uses the photomultipliers (H8259, H8259-01 and H8259-02, Hamamatsu), which cover the spectrum range from 185 to 900 nm.

The spectrum of upconversion luminescence under excitation of the crystals ZrO_2-13.4mol.%Y_2O_3-0.6mol.%Ho_2O_3 by radiation of the thulium fiber laser of the wavelength of 1940 nm was recorded using the spectrometer based on the Horiba 1000 monochromator. The luminescence was recorded by the Hamamatsu R928 PMT.

The images of the „burn ups" at the butt ends of the active elements after the generation experiment were obtained using the optical microscope Carl Zeiss Axio Imager Z2 Vario.

Results and discussion

The oxygen vacancy in zirconium dioxide is an amphoteric defect for charge localization. Thus, the number of the electrons captured by this defect will affect the position of

the energy levels of the respective defect in the band gap of the crystal. The experimental and theoretical studies for determination of the position of the energy levels related to the oxygen vacancies in the zirconium dioxide crystals are described in the papers [10–14,18,19]. It should be noted that the experimental studies of the paper [13] were performed on the crystals of nonstoichiometric zirconium dioxide with a monoclinic structure.

Using the spin-polarization density functional theory, the authors of [12] have calculated the band gap width and investigated an electron structure of the oxygen vacancies in the monoclinic, tetragonal and cubic phases. And for the monoclinic crystals ZrO_2, too, the paper [12] has determined the Kohn-Sham levels localized in the band gap, for the three $(3f)$ and four $(4f)$ oxygen vacancies in the five charged states.

Using the spectrum-luminescence methods and the quantum-chemistry calculations, the paper [13] has identified the mechanisms of a luminescence band with the maximum of 2.7 eV appearing under excitation by radiation of the energy of 5.2 eV in the crystals of monoclinic zirconium dioxide. Using the quantum-chemistry simulation, the authors of [13] have obtained a diagram of the single-electron Kohn-Sham levels in the band gap of the monoclinic crystal ZrO_2 for the three- and four-coordinated oxygen vacancies (V^0) in the various charged states.

The present paper has investigated the spectroscopic characteristics of the crystals of stabilized zirconium dioxide ZrO_2-13.6mol.%Y_2O_3-0.4mol.%Ho_2O_3, ZrO_2-13.4mol.%Y_2O_3-0.6mol.%Er_2O_3, ZrO_2-15mol.%Y_2O_3, which are characterized by the cubic structure, when they are excited by synchrotron radiation, in order to identify the luminescence bands due to the defects related to the oxygen vacancies.

Fig. 2, *a* shows the low-temperature luminescence spectra of the crystals ZrO_2-13.6mol.%Y_2O_3-0.4mol.%Ho_2O_3 under excitation by synchrotron radiation with the energies of 4.8, 5.05, 5.61, 6.01 eV. The luminescence spectrum is represented by a wide band of the maximum of ~ 478 nm and narrow lines against its background, which correspond to the transitions $^5F_4$, $^5S_2 \rightarrow {}^5I_8$ of the ions Ho^{3+}. No change in the shape of the luminescence spectrum profiles is observed for change of the excitation energy. „Dips“ in the form of the narrow lines within the region of $415-490$ nm in the spectrum of wideband luminescence are the result of reabsorption of radiation of wideband luminescence by the ions Ho^{3+}. The analysis of the literature data has found that the spectrum of wideband luminescence with the maximum near 478 nm, as specified in [13], was due to structure defects, related to the oxygen vacancies, in the monoclinic crystals ZrO_2 of the nonstoichiometric composition. As the crystals investigated in the present paper have the oxygen vacancies in the structure due to the heterovalent substitution of the ions Zr^{4+} with the ions Y^{3+} and Ho^{3+}, we have concluded that the wide band in the luminescence spectrum of the crystals
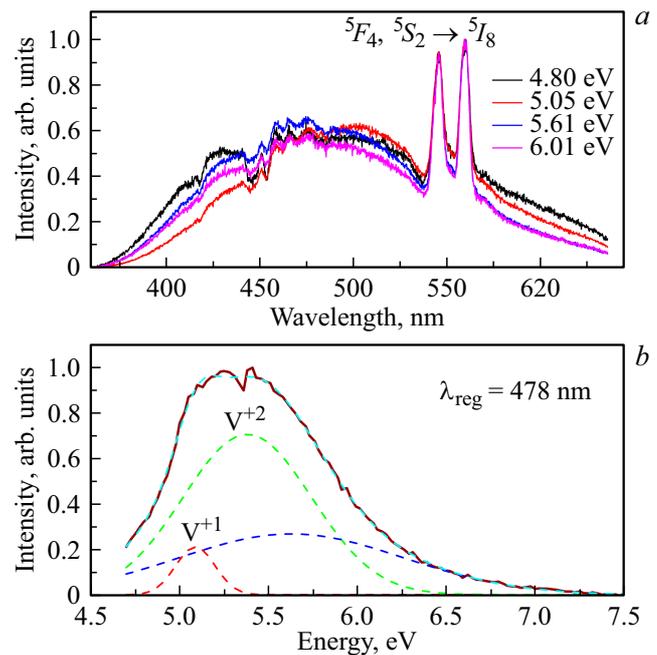
Figure 2. (*a*) Luminescence spectra of the crystals ZrO_2-13.6mol.%Y_2O_3-0.4mol.%Ho_2O_3 under excitation by synchrotron radiation of the energy of 4.8, 5.05, 5.61, 6.06 eV ($T = 10$ K); (*b*) the excitation spectra observed at radiation of $\lambda_{reg} = 478$ nm ($T = 10$ K).

ZrO_2-13.6mol.%Y_2O_3-0.4mol.%Ho_2O_3 also corresponded to luminescence of defects related to the oxygen vacancies.

Fig. 2, *b* shows the excitation spectrum of the crystals ZrO_2-13.6mol.%Y_2O_3-0.4mol.%Ho_2O_3, which is obtained at the luminescence recording's wavelength of 478 nm. This figure indicates that the profile of the excitation spectrum is asymmetrically shaped, which, as we believe, is the result of superposition of the bands, which are due to transition of the electrons from the valence band into the energy levels of various defects (related to the oxygen vacancies) and to the valence band — conduction band transition.

In accordance with the simulation results [10–14], the vacancies V^{+1} and V^{+2} are characterized by electron-unfilled energy levels near the conduction band's bottom (within the region of $5-5.5$ eV). In accordance with it, the complex profile of the excitation spectrum (Fig. 2, *b*) was presented as superposition of individual bands. The best compliance between the experimental and the approximating profiles has been obtained for the Gaussian profiles with the maxima corresponding to the values 5.1, 5.4 and 5.6 eV.

We have attributed the bands with the maxima of 5.1 and 5.4 eV to electron transitions from the valence band to the energy levels of defects related to the oxygen vacancies V^{+1} and V^{+2}. The paper [12] has noted that the crystals of stabilized zirconium dioxide were characterized by poly-vacancies resulting from interaction of the nearest oxygen vacancies. This interaction results in overlapping of the defect levels and appearance of the wide band of the defect
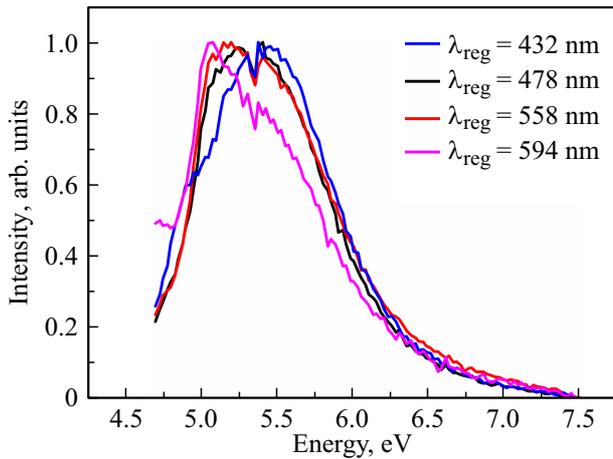
Figure 3. Spectrum of crystal excitation ZrO_2-13.6mol.%Y_2O_3-0.4mol.%Ho_2O_3, λ_{reg} = 432, 478, 558, 594 nm, $T = 10$ K.
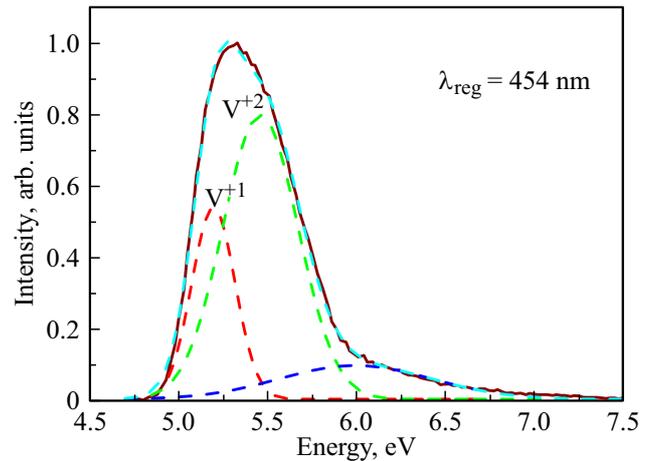
Figure 5. Excitation spectrum of the crystals ZrO_2-13.4mol.%Y_2O_3-0.6mol.%Er_2O_3, as observed at radiation of λ_{reg} = 454 nm, $T = 10$ K.
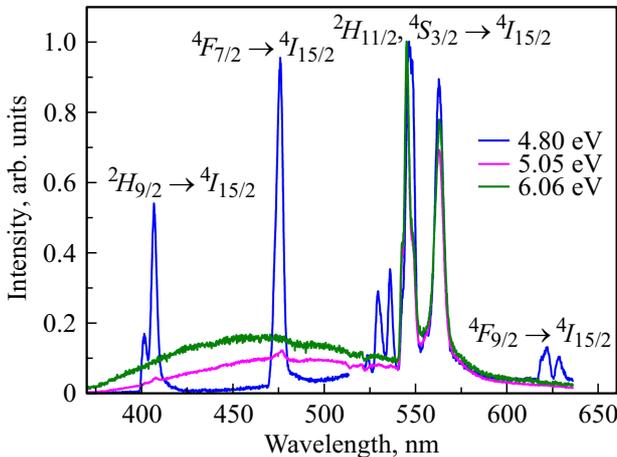
Figure 4. Spectra of luminescence of the crystals ZrO_2-13.4mol.%Y_2O_3-0.6mol.%Er_2O_3 under excitation by synchrotron radiation of the energy of E_{exc} = 4.8, 5.05, 6.06 eV, $T = 10$ K.

energies [12]. Therefore, based on the excitation spectra and the luminescence spectra that are typical for these crystals, it is quite difficult to unambiguously determine the energy value corresponding to the valence band — the conduction band transition. Therefore, the band with the maximum of 5.6 eV in the excitation spectra is, we believe, the result of a combination of the electron transitions from the valence band to the conduction band and the transitions to the defects' energy level near the conduction band's bottom (the band consisting in closely spaced energy levels, which is due to generation of a polyvacancy).

The fact that the wide-band luminescence spectra of Fig. 2, *a* are a superposition of the luminescence spectra for the structure defects characterized by a different position of the energy levels, is indicated by a shift of the maximum of the excitation spectrum profile when recording at the luminescence wavelengths of 432, 478, 558, 594 nm (Fig. 3).

The structure defects related to the oxygen vacancies in the crystals of stabilized zirconium dioxide with the cubic structure have been identified via additional studies of the spectrum-luminescence characteristic of the crystals ZrO_2-13.4mol.%Y_2O_3-0.6mol.%Er_2O_3 and ZrO_2-15mol.%Y_2O_3 under excitation thereof by synchrotron radiation. Fig. 4 shows the low-temperature luminescence spectra of the crystals ZrO_2-13.4mol.%Y_2O_3-0.6mol%Er_2O_3 under excitation thereof by synchrotron radiation with the energies of E_{exc} = 4.8, 5.05, 6.06 eV.

In the same way as for the crystals ZrO_2-13.6mol.%Y_2O_3-0.4mol.%Ho_2O_3, the luminescence spectrum of the crystals of stabilized zirconium dioxide ZrO_2-13.4mol.%Y_2O_3-0.6mol.%Er_2O_3 is represented by the wide band with the maximum of ~ 454 nm, whose background has visible lines due to the transitions $^2H_{9/2} \rightarrow {}^4I_{15/2}$, $^4F_{7/2} \rightarrow {}^4I_{15/2}$, $^2H_{11/2}$, $^4S_{3/2} \rightarrow {}^4I_{15/2}$, $^4F_{9/2} \rightarrow {}^4I_{15/2}$ of the ions Er^{3+} (Fig. 4).

It should be noted that the luminescence spectra exhibit the lines due to the transitions $^2H_{9/2} \rightarrow {}^4I_{15/2}$, $^4F_{7/2} \rightarrow {}^4I_{15/2}$, $^4F_{9/2} \rightarrow {}^4I_{15/2}$ of the ions Er^{3+} at the excitation energies within the range of 4.7−5.0 eV. With these excitation energies, the relative intensity of the defect-caused wide band in the luminescence spectra within the range of 380−600 nm is less (Fig. 4) than for the similar excitation energies in the luminescence spectra of the crystals ZrO_2-13.6mol.%Y_2O_3-0.4mol.%Ho_2O_3 (Fig. 2, *a*). With increase in the excitation energy (≥ 6 eV), the relative intensity of the defect-caused wide band increases. In this excitation method, no line corresponding to luminescence due to the transitions from the levels $^2H_{9/2}$, $^4F_{7/2}$, $^4F_{9/2}$ to the ground multiplet $^4I_{15/2}$ of the ions Er^{3+} has been detected. At the same time, there are only the lines due to the transition $^2H_{11/2}$, $^4S_{3/2} \rightarrow {}^4I_{15/2}$. Based thereon, it has been concluded that the in the crystals of zirconium dioxide alloyed with erbium ions, with the excitation energies within the region of 4.7−5.0 eV, the most effective excitation is in the energy
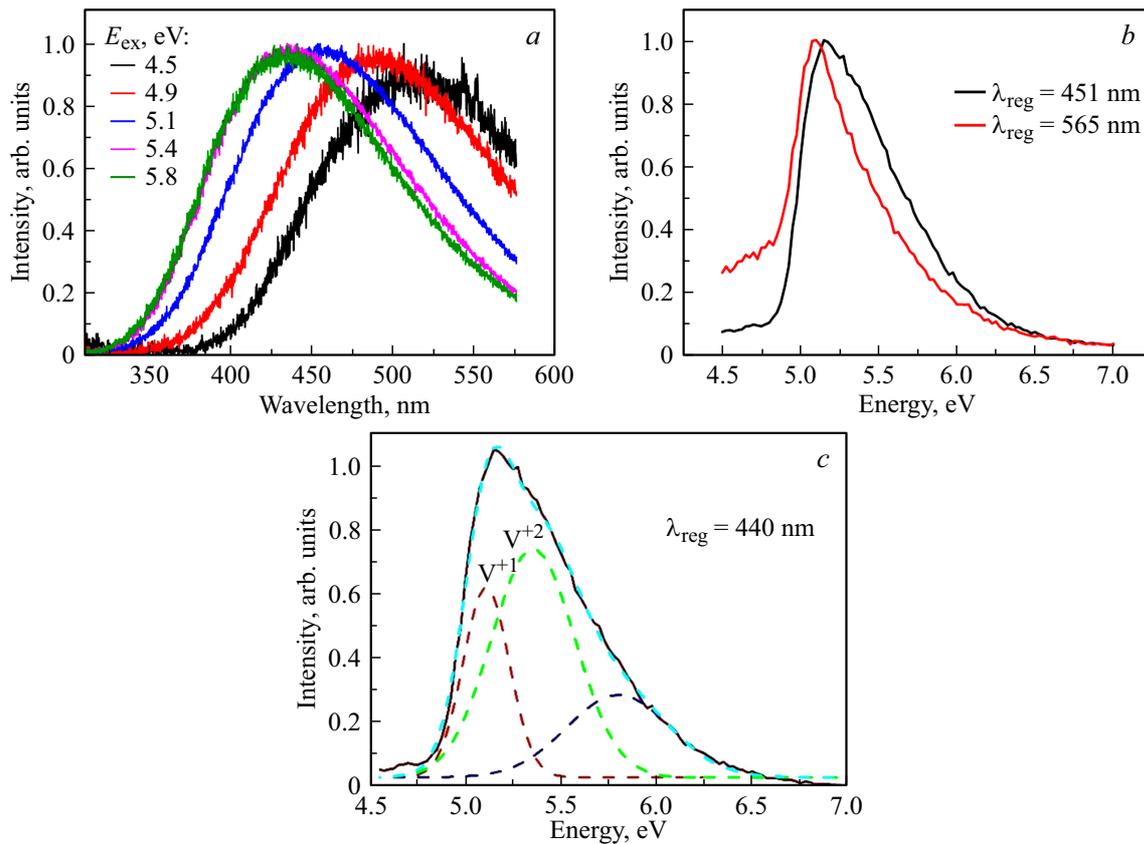
Figure 6. (*a*) Luminescence spectra of the crystals ZrO_2-15mol.%Y_2O_3 under excitation by synchrotron radiation of the energy of $E_{exc} = 4.5, 4.9, 5.1, 5.4, 5.8$ eV, $T = 10$ K, (*b*) Excitation spectra of the crystals ZrO_2-15mol.%Y_2O_3 observed at radiation with $\lambda_{reg} = 451$, 565 nm, $T = 10$ K, (*c*) Excitation spectra of the crystals ZrO_2-15mol.%Y_2O_3 observed at radiation with $\lambda_{reg} = 440$ nm.

levels of the ions Er^{3+}, while with the excitation energies of ≥ 6 eV, the most effective excitation is in the defect levels, from which the energy is non-radiatively transferred to the ions Er^{3+} thereafter.

Fig. 5, *b* shows the excitation spectrum of the crystals ZrO_2-13.4mol.%Y_2O_3-0.6mol.%Ho_2O_3, which is obtained at the luminescence recording's wavelength of 454 nm. This spectrum has been analyzed to indicate a complex nature of the profile. It results from the superposition of the bands of the electron transitions from the valence band to the band gap's energy levels of the defects related to the oxygen vacancies and the band generated due to the combination of the valence band–conduction band transitions and the transitions to the energy levels of the defects near the conduction band bottom (it is a band consisting in the closely spaced energy levels, which is due to generation of the polyvacancy).

Three bands with the maxima of 5.2, 5.5 and 6 eV have been obtained in decomposition of the complex profile into the Gaussian components. Similar to the above discussions, the bands with the maxima of 5.2 and 5.5 eV can be related to the electron transitions from the valence band to the energy levels of the oxygen vacancies V^{+1} and V^{+2}. The band with the maximum of 6 eV is due

to the valence band–conduction band transition and the transitions to the energy levels of the defects related to generation of the polyvacancies near the conduction band's bottom.

The similar studies of the excitation and luminescence spectra have been performed for the RE ion-undoped crystals of zirconium dioxide stabilized by yttrium oxide ZrO_2-15mol.%Y_2O_3. Fig. 6 shows respective luminescence spectra of the crystals ZrO_2-15mol.%Y_2O_3 under excitation thereof by synchrotron radiation of the energy of $E_{exc} = 4.5$, 4.9, 5.1, 5.4, 5.8 eV, as well as the crystal excitation spectra observed at $\lambda_{reg} = 451$, 565 and 440 nm.

The luminescence spectra Fig. 6, *a* have been analyzed to indicate the change of the position of the luminescence maximum depending on the excitation energy, thereby possibly indicating the presence of various kinds of defects (Fig. 6, *b*). The bands corresponding to the two kinds of the defects V^{+1} and V^{+2} with the energies of 5.1 and 5.4 eV. The band with the maximum of 5.8 eV results from the superposition of the bands which result from the electron transitions to the energy levels of the defects near the conduction band and from the valence band–conduction band transitions.

Energies corresponding to the position of the maximums in decomposition of the excitation spectra of the crystals into the Gaussian components ZrO_2-13.6mol.%Y_2O_3-0.4mol.%Ho_2O_3, ZrO_2-13.4mol.%Y_2O_3-0.6mol.%Er_2O_3, ZrO_2-15mol.%Y_2O_3.

Positions of the maxima of the bands	V^{+1}	V^{+2}	E_{g+pvk}
ZrO_2-13.6mol.%Y_2O_3-0.4mol.%Ho_2O_3	5.1	5.4	5.6
ZrO_2-13.4mol.%Y_2O_3-0.6mol.%Er_2O_3	5.2	5.5	6
ZrO_2-15mol.%Y_2O_3	5.1	5.5	5.8
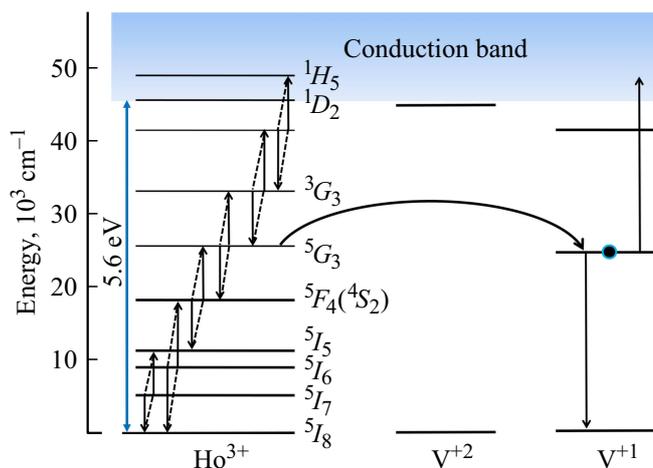
Figure 7. Diagram for the processes of nonradiative transfer of the energy between the ions Ho^{3+} and the structure defects due to the oxygen vacancies in the crystals ZrO_2-13.6mol.%Y_2O_3-0.4mol.%Ho_2O_3.

The results obtained from the excitation spectra for the crystals ZrO_2-13.6mol.%Y_2O_3-0.4mol.%Ho_2O_3, ZrO_2-13.4mol.%Y_2O_3-0.6mol.%Er_2O_3, ZrO_2-15mol.%Y_2O_3, are tabularized.

It should be noted that in accordance with the literature data [10–14], along with the electron-unfilled energy level near the conduction band's bottom (as identified in the present paper), the defect V^{+1} is also characterized by the energy level with the electron thereon near the band gap middle. The energy levels with the electrons thereon are also typical for the vacancies V^0, V^{-1}, V^{-2}. However, the research of the spectrum-luminescence characteristics of these defects requires other excitation sources, so these studies have not been included in the present paper. At the same time, the defects V^0, V^{-1}, V^{-2} can not be omitted in areas near the butt ends (the butt ends are an interface, where the number of the defects is the biggest) of the active elements of the crystals ZrO_2-13.6mol.%Y_2O_3-0.4mol.%Ho_2O_3.

In accordance with the above-described results, the diagram demonstrating appearance of the electrons in the conduction band of the crystals ZrO_2-13.6mol.%Y_2O_3-0.4mol.%Ho_2O_3, is shown on Fig. 7.

The presence of interaction of the excited ions Ho^{3+} in the crystals is indicated by the upconversion luminescence spectra due to the transitions $^5I_6 \rightarrow {}^5I_8$, $^5F_4 \rightarrow {}^5I_8$, $^5F_5 \rightarrow {}^5I_8$ of the ions Ho^{3+} under excitation thereof to the level $^5I_7$ (Fig. 8, a, b) as per the diagram (Fig. 8, c).

Conclusion

Using synchrotron radiation as an excitation source, the spectrum-luminescence methods have been taken to identify the structure defects of the crystals ZrO_2-Y_2O_3-Ho_2O_3, ZrO_2-Y_2O_3-Er_2O_3, ZrO_2-Y_2O_3, which are due to the oxygen vacancies. The obtained excitation and luminescence spectra of the crystals of stabilized zirconium dioxide made it possible to determine the positions of the energy levels of the oxygen vacancies V^{+1} and V^{+2} near the conduction band.

The experimental results obtained in the paper indicate that the reduction of beam stability of the crystals of stabilized zirconium dioxide that are doped with RE ions can be related to the oxygen vacancies therein which occur due to heterovalent substitution of the ions Zr^{4+} with the ions Y^{3+}, as well as due to RE elements therein.

Acknowledgments

Conflict of interest

The authors declare that they have no conflict of interest.

References

[1] P.A. Ryabochkina, M.A. Borik, E.E. Lomonova, A.V. Kulebyakin, F.O. Milovitch, V.A. Myzina, N.Yu. Tabachkova, N.V. Sidorova, A.N. Chabushkin. FTT, **57** (8), 1549 (2015) (in Russian).

[2] P.A. Ryabochkina, N.V. Sidorova, A.N. Chabushkin, E.E. Lomonova. Quant. Electron., **46** (5), 451 (2016). DOI: 10.1070/QEL15933

[3] V.E. Shukshin. Trudy IOFRAN, **64**, 3 (2008) (in Russian).

[4] M.N. Khromov. *Lazery na kristallakh s razuporyadochennoi strukturoi s diodnoi nakachkoi.* Avtoref. kand. dis. (Institut obshchei fiziki im. A.M. Prokhorova, M., 2009) (in Rusian).

[5] M.A. Borik, E.E. Lomonova, A.V. Malov, A.V. Kulebyakin, P.A. Ryabochkina, S.N. Ushakov, M.A. Uslamina, A.N. Chabushkin. Quant. Electron., **42** (7), 580 (2012). DOI: 10.1070/QE2012v042n07ABEH014867
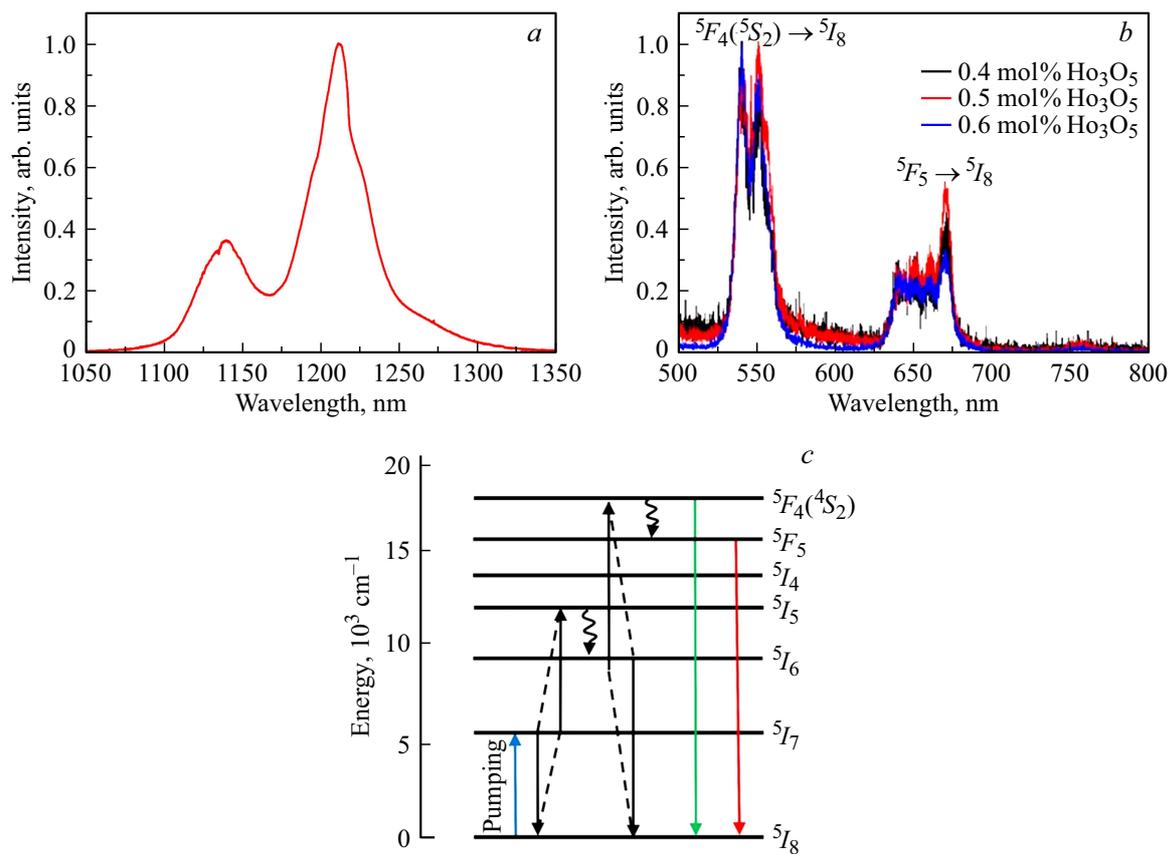
Figure 8. Upconversion luminescence spectra due to the transitions (*a*) $^5I_6 \rightarrow {}^5I_8$, (*b*) $^5F_4 \rightarrow {}^5I_8$, $^5F_5 \rightarrow {}^5I_8$, as recorded under excitation by the laser radiation of $\lambda_{exc} = 1940\,\text{nm}$, (*c*) Diagram of the energy levels of the ions Ho^{3+} with indicated processes of interionic interaction of the ions Ho^{3+} which provide upconversion luminescence of the ions Ho^{3+}, for the transitions $^5I_6 \rightarrow {}^5I_8$, $^5F_4$, $^5S_2 \rightarrow {}^5I_8$, $^5F_5 \rightarrow {}^5I_8$ In crystals ZrO_2-13.6mol.%Y_2O_3-0.4mol.%Ho_2O_3.

[6] M.A. Borik, E.E. Lomonova, A.A. Lyapin, A.V. Kulebyakin, P.A. Ryabochkina, S.N. Ushakov, A.N. Chabushkin. Quant. Electron., **43** (9), 838 (2013). DOI: 10.1070/QE2013v043n09ABEH015258

[7] S.A. Artemov, A.N. Chabushkin, A.A. Lyapin, P.A. Ryabochkina, O.L. Antipov, E.E. Lomonova. Laser Physics, **28** (3), 035803 (2018). DOI: 10.1088/1555-6611/aa962f.

[8] S.A. Artemov, E.A. Artemov, E.E. Lomonova, P.A. Ryabochkina, A.N. Chabushkin. Quant. Electron., **51** (7), 586 (2021). DOI: 10.1070/QEL17592

[9] S.A. Artemov. *Vliyanie defectov structury na kharakteristiki dvukhmironnoi lazernoi generatsii na kristallakh ZrO₂-Y₂O₃-Ho₂O₃. Avtoref. kand. dis.* (FGBOU VO „Natsionalnyi issledovatelskii Mordovskii gosudarstvennyi universitet im. N.P. Ogareva", Saransk, 2022) (in Russian).

[10] A.S. Foster, V.B. Sulimov, F.L. Gejo, A.L. Shluger, R.M. Nieminen. Phys. Rev. B, **64**, 224108 (2001). DOI: 10.1103/PhysRevB.64.224108

[11] J.-H. Hur, S. Park, U.I. Chung. J. Appl. Phys., **112** (11), 113719(2012). DOI: 10.1063/1.4768894.

[12] T.V. Perevalov, D.R. Islamov. ECS Transactions, **80** (1), 357 (2017). DOI: 10.1149/08001.0357ecst

[13] D.R. Islamov, V.A. Gritsenko, T.V. Perevalov, A.P. Yelisseyev, V.A. Pustovarov, I.V. Korolkov, E.E. Lomonova. Materialia, **15**, 100979 (2021). DOI: 10.1016/j.mtla.2020.100979

[14] C. Arhammar, C.M. Araujo, R. Ahuja. Phys. Rev. B, **80**, 115208 (2009). DOI: 10.1103/PhysRevB.80.115208

[15] K. Chernenko, A. Kivimäki, R. Pärna, W. Wang, R. Sankari, M. Leandersson, H. Tarawneh, V. Pankratov, M. Kook, E. Kukk, L. Reisberg, S. Urpelainen, T. Käämbre, F. Siewert, G. Gwalt, A. Sokolov, S. Lemke, S. Alimov, J. Knedel, O. Kutz, T. Seliger, M. Valden, M. Hirsimäki, M. Kirm, M. Huttula. J. Synchr. Rad., **28**, 1620 (2021). DOI:10.1107/S1600577521006032

[16] V. Pankratov, A. Kotlov. Nucl. Instr. Meth. Phys. Res. B, **474**, 35 (2020). DOI: 10.1016/j.nimb.2020.04.015

[17] V. Pankratov, R. Pärna, M. Kirm, V. Nagirnyi, E. Nõmmiste, S. Omelkov, S. Vielhauer, K. Chernenko, L. Reisberg, P. Turunen, A. Kivimäki, E. Kukk, M. Valden, M. Huttula. Radiation Measur., **121**, 91 (2019). DOI: 10.1016/j.radmeas.2018.12.011

[18] P.J. Shen, S.P. Jiang, K.P. Ong, W.Z. Ding, P.-I. Mao, X.G. Lu, C.H. Li, P. Wu. J. Alloys and Comp., **506** (2), 898 (2010). DOI: https:10.1016/j.jallcom.2010.07.108

[19] R.H. French, S.J. Glass, F.S. Ohuchi, Y.-N. Xu, W.Y. Ching. Phys. Rev. B, **49**, 5133 (1994). DOI: 10.1103/PhysRevB.49.5133

Translated by M.Shevelev